

Improving Ductility of Sprayed Fire Resistant Materials

Major Qualifying Project Report



Presented by:

John DeVine, Jr.

Presented to:

Professor Nima Rahbar and the Worcester Polytechnic Institute Civil Engineering Department in partial fulfillment of the requirements for the Degree of Bachelor of Science

2017-2018

Executive Summary

Structural steel is widely used in building construction. However, a steep decrease in the yield strength and elastic modulus of steel at high temperatures can cause a structural failure. To combat the poor performance of steel at high temperatures, many codes require the use of passive fire protection by means of a sprayed fire resistant material (SFRM). SFRMs are a type of lightweight concrete applied to exposed steel that possesses a low thermal conductivity, which is pivotal in limiting the temperature of the protected steel to safe levels. The low cost and fast and easy application of SFRMs make them widely used as passive fire protection in steel structures.

Though density and thermal conductivity of commercially available SFRMs are both at acceptable levels, many SFRMs fall flat in other aspects of performance. The two largest problems with current SFRMs is their strength/brittleness and their adhesive properties to steel. As a type of concrete, SFRMs perform very poorly in flexural strength and deflection; testing shows that a normal SFRM has a tensile strength below 0.1 MPa and a tensile strain capacity of less than 0.01%. As the SFRM is subjected to high loads from events like earthquakes or explosions, it will break and start to partially delaminate from steel. Heat from a fire can then penetrate through the delamination and heat the steel directly, severely hindering the efficacy of the SFRM. Partial delamination of the SFRM can decrease failure time by up to 36% in a structure. Because heavy loads emanating from earthquakes or explosions can severely damage an active fire protection system in a structure, it is pivotal for the SFRM to perform well, as it is often the last line of defense for a structure from fire.

The purpose of this study is to combat delamination occurring from the brittle nature of commercially available SFRMs. To lessen the effects of the inherent brittleness of concrete, fibers can be introduced into the mix to make a fiber reinforced concrete (FRC). FRCs come in two different categories: conventional FRCs and high ductility FRCs. In a conventional FRC, fibers bridge the distance between the cracks and allow further cracking in the concrete to occur. However, the stress held in subsequent cracks does not reach the magnitude of the stress held by the fibers in the first crack. This gives a conventional FRC strain-softening behavior. A high ductility FRC has fibers that bridge the cracks as well; the difference between them is the strain-hardening behavior of the high ductility FRC. Additional strain of the composite requires additional load in a high ductility FRC, which improves its flexural performance. High ductility FRCs have been developed as SFRMs with a density of 550 kg/m³, a first crack strength of 0.87 MPa, and a ductility of 3%. Though promising, these numbers can still be improved upon. The goal of this study is to create a high performance FRC with thermal properties similar to commercially available SFRMs in order to create an SFRM that is less susceptible to delamination.

Besides ordinary portland cement and water, the materials used in the proposed SFRM were nylon fibers, vermiculite, and sodium bentonite. Nylon fibers were chosen over other fibers used in FRCs (high tenacity polypropylene, polyvinyl alcohol) because of its relatively high elastic modulus. This allows for a larger crack width in the concrete, which in turn contributes to a higher ductility. Nylon fibers were chosen over the alternate options despite their lower ultimate strength and frictional sliding shear stress; the improvements from the increased elastic modulus were shown to outweigh the benefits of a higher ultimate strength and frictional sliding shear stress of the other fibers. Vermiculite acts as a lightweight aggregate for the concrete. The accordion-like structure of vermiculite gives the cement a larger bonding surface area, which increases the overall strength of the cement-aggregate bonds. This leads to a higher first crack strength of the concrete. Vermiculite also has a low thermal conductivity (~ 0.06 W/mK), which is an ideal property for an aggregate to have when used in the design of SFRMs. Sodium bentonite is a type of smectite clay that provides insulation properties to the SFRM as well as increases workability and fiber dispersion in the mix. Four different concrete mixes were synthesized over the course of the project. Each mix had equivalent proportions of cement, sodium bentonite, vermiculite, and fibers. The amount of water used in each mix varied in order to find an optimal first crack strength.

The mechanical results of the study showed that the addition of fibers into the mix greatly improved its flexural performance. First crack strength of the concretes ranged from 0.523 MPa to 1.575 MPa, which far outperforms a typical SFRM with a tensile stress capacity of 0.1 MPa. The maximum strain capacity of the four mixes ranged between 0.307% and 0.385%, which is an order of magnitude better than standard SFRMs. Analysis of stress-strain curves showed that the concrete went through four main stages before failure. Phase I was an elastic deformation of the concrete due to applied load. Phase II was a steep decrease in stress capacity due to the first crack in the concrete. After Phase II, the concrete itself had no tensile stress capacity; the nylon fibers that bridged the crack held the tensile stress. During Phase III, the fibers elastically deformed and allowed the specimen to deform even more. Phase III saw a gradual increase in stress capacity until the beginning of Phase IV, where the fibers changed from elastic deformation to plastic deformation and eventual rupture.

Though mechanical results from the study of the four mixes were far better than a typical SFRM, the specimens tested were not characteristic of a high ductility FRC. Rather, they mirrored the characteristics of a conventional FRC. In order to get more optimal results in the future, more fibers would need to be added so that the stress capacity in Phase II is not as severe. This would allow the fibers to hold enough stress to where the concrete would reach cracking stress again. The advent of multiple cracking in the concrete would increase its deflection and therefore increase its ductility.

Authorship

All components of the report were performed and written by John DeVine, Jr.

Acknowledgements

I would like to thank **Professor Nima Rahbar** for his invaluable help, advice, and guidance as my advisor over the course of my concrete mix design, report writing, and scholarly article writing.

I would like to thank **Fabio Mazza** for the work he performed on the project before I began working on it; his initial design laid the groundwork for this report.

I would like to thank **Professor Tahar El-Korchi** for his guidance in scholarly article writing for this project.

Lastly, I would like to thank **the professors in the WPI Civil Engineering Department** for teaching me the last four years and helping me acquire the knowledge necessary to finish this report.

Table of Contents

Executive Summary 2

Authorship..... 4

Acknowledgements..... 5

Table of Contents 6

Abstract..... 7

1.0 Background..... 8

 1.1 SFRM Overview 8

 1.2 Problems with SFRMs 10

 1.3 SFRM Performance after Partial Delamination..... 12

 1.4 Introduction to Thermal Conductivity in Concretes 13

 1.5 SFRM Standardized Performance Tests 14

 1.6 Introduction to Fiber Reinforced Concrete (FRC) 16

2.0 Concrete Materials 20

 2.1 Lightweight Aggregates 20

 2.2 Fibers 22

 2.3 Sodium Bentonite 22

3.0 Methods 24

 3.1 Concrete Mix Design 24

 3.2 Mechanical Testing 25

 3.3 Computation of Stress-Strain Curves 25

4.0 Results..... 28

 4.1 Mix 1 Results..... 28

 4.2 Mix 2 Results..... 29

 4.3 Mix 3 Results..... 30

 4.4 Mix 4 Results..... 30

 4.5 Results Summary..... 31

5.0 Discussion..... 33

 5.1 Mechanical Results Discussion..... 33

 5.2 Expected Thermal Results Discussion 34

6.0 Conclusion 35

7.0 References 36

Abstract

Sprayed fire resistant materials (SFRMs) are widely used as passive fire protection for steel construction. As a type of concrete, they are inherently brittle. SFRMs can therefore delaminate from steel due to service loads or impact loads, creating gaps through which heat can penetrate, rendering the SFRM useless. A new class of SFRMs was proposed in this study that uses nylon fibers to create a fiber reinforced concrete (FRC). The SFRMs synthesized over the course of the study had first crack strengths 5-15 times greater than typical SFRMs and tensile strain capacities 30-40 times greater than typical SFRMs. The strain capacities could be greatly improved upon in future testing by increasing the volume of fibers in the SFRM, which would foster a strain-hardening behavior in the material.

1.0 Background

1.1 SFRM Overview

Structural steel is widely used in building construction. However, the strength of steel decreases when exposed to high temperatures. Therefore, in the case of a fire, the elastic modulus and yield strength of steel decreases. Figure 1.1 below shows the relationship between temperature the yield strength of steel relative to its strength at room temperature [1].

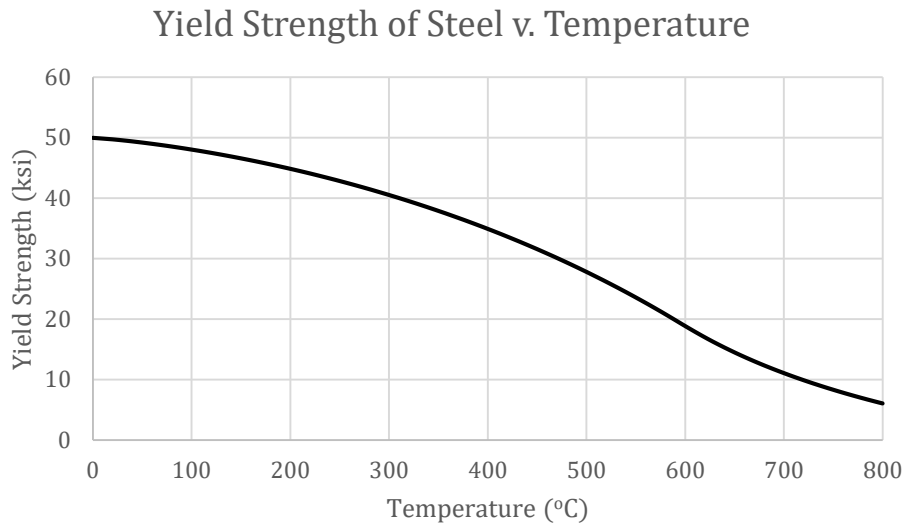


Figure 1.1 [1] shows the relationship between steel yield strength and temperature.

As shown in the graph, the yield strength of steel can decrease over 60% when it reached 600°C. A decrease in the material properties of steel can lead to structural failure. In order to combat the failure of steel at high temperatures, sprayed fire-resistant materials (SFRMs) are applied to steel. SFRMs are a type of cementitious or gypsum-based material that is applied to exposed steel beams in order to protect them from high temperatures emanating from a fire. A high-performing SFRM has a low thermal conductivity, which delays the temperature increase of the steel, and a relatively low density, which reduces the load on the beam it is applied to. Its low thermal conductivity delays the time to structural failure of the building. SFRMs are widely used to protect steel for multiple reasons: SFRMs are inexpensive, relatively easy to apply (due to its lightweight and ability to be sprayed), and can be applied to a structure quickly.

There are two main categories of SFRMs: wet mix and dry mix. The main difference between the two is the point at which water is introduced to the concrete mix. In a wet mix

SFRM, water is premixed with the cement and aggregates before being applied to concrete so that the SFRM can be sprayed like a liquid onto the steel. A dry mix SFRM, however, is mixed with water the instant before spraying the SFRM onto steel. The water and aggregate powder is mixed in the nozzle of the sprayer right before their application to steel [2]. SFRMs are commonly comprised of cementitious materials and other lightweight components (perlite, vermiculite, etc.). These materials are widely used because of their very low density and low thermal conductivity, as an ideal SFRM is a lightweight insulator. Figure 1.1 below shows the thermal performance of three SFRMs currently on the market [3].

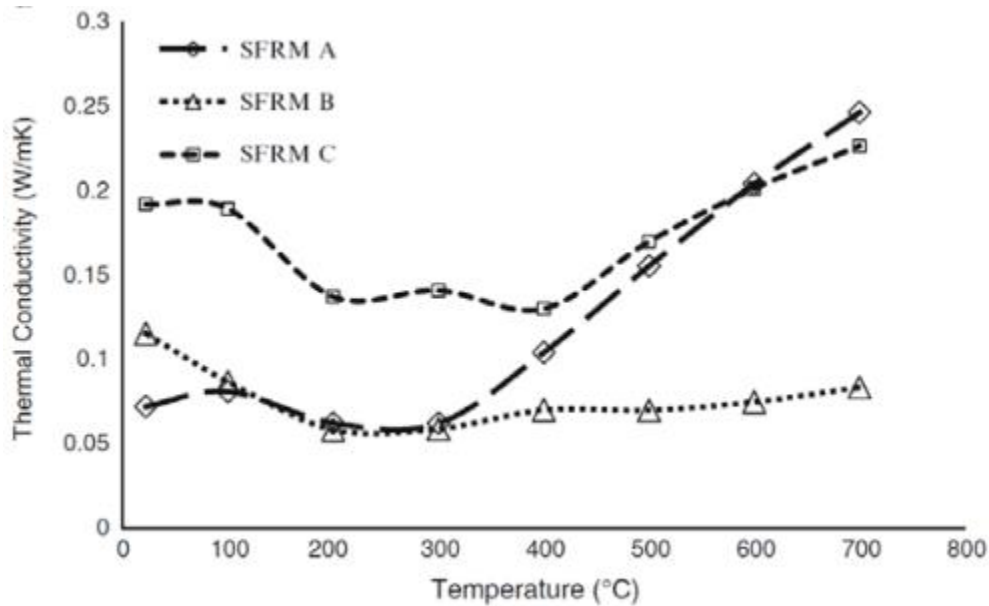


Figure 1.2 [3] shows the relationship between thermal conductivity and temperature of three SFRMs currently available.

As shown by Figure 1.2, current SFRMs range between 0.07 W/mK and 0.19 W/mK at room temperature and 0.08 W/mK and 0.25 W/mK at 700°C. The graph clearly shows that SFRM B is the most successful from an insulating standpoint, as its thermal conductivity stays below 0.1 W/mK at temperatures above 100°C, whereas the thermal conductivity of the other two SFRMs increase to between 0.2 and 0.25 W/mK at high temperatures.

As stated above, SFRMs need to be relatively light. An SFRM that is not dense is easier to apply because it is easier to transport. A light SFRM is also preferable to put the lowest possible dead load on a structure. Table 1.1 shows the densities of the three SFRMs that were tested for thermal conductivity [3].

Insulation Type	Room Temperature Density (kg/m ³)	Density at 700°C (kg/m ³)	Decrease in Density
SFRM A	298	241.3	19.0%
SFRM B	423.2	349.8	17.3%
SFRM C	451.8	349.8	15.6%

Table 1.1 shows the densities of the three SFRMs at room temperature and at 700°C, along with the decrease in density percentage.

This table shows that SFRMs are expected to decrease in density between 15% and 20% when exposed to high heat. It also displays a normal range of densities for standard SFRMs. SFRMs typically come in two density classes. A low density SFRM has a density between 240 kg/m³ and 320 kg/m³, whereas a medium density SFRM has a density between 320 kg/m³ and 640 kg/m³. These are both very light when compared to normal weight structural concrete, which is typically over 2,000 kg/m³. Density of the SFRM correlates with its strength and durability. A low density SFRM is more likely to be applied to indoor surfaces, whereas a medium density SFRM is typically sprayed on steel beams that are exposed to weather exposed surfaces.

The importance of SFRMs cannot be understated in the construction of many steel structures. Certain provisions in building codes and FM Global Data Sheets advise or require the use of fireproofing spray. In general, currently manufactured SFRMs accomplish their task of insulating steel while maintaining a very low density when compared to normal concrete.

1.2 Problems with SFRMs

Though current SFRMs perform well when it comes to density and thermal conductivity, many SFRMs struggle in other aspects of performance. The two main concerns are SFRMs adhesion to the beams it covers and the strength/brittleness of the material. Significant impact damage or earthquake are known problems for SFRMs and can severely hinder their performance in the case of a fire.

Though during normal use, an SFRM performs as expected, heavy impact on a building can cause an SFRM to fail [4, 5]. An example of impact on a building negatively affecting the performance of an SFRM was during the attacks on September 11, 2001. Heavy impact on the towers due to aircraft caused the SFRMs to be dislodged from the building, which caused the structure to weaken and eventually collapse. NIST’s report noted that “dislodgement could occur as a result of direct impact by debris or due to inertial forces as a

result of the aircraft impact.” It mentions that even parts of the building that were not directly hit by aircraft saw their SFRMs dislodge. Once again, this shows how poor adhesion of the SFRMs can lead to the catastrophic failure of a building. The report states that in order to improve the efficacy of SFRMs in the future, they should be tested for durability when subjected to vibration, abrasion, shock, and temperature fluctuations.

The report also raises concerns about the failure of SFRMs during normal service loads. SFRMs are subject to deterioration and delamination failure. As mentioned in the report, “Adhesion failures were common, likely because of the exposed conditions of the columns and inherently low strength of the SFRM.” This one sentence outlines possibly the largest problem with current day SFRMs: low strength and relatively poor adhesion causes them to perform poorly. Testing of currently available SFRMs shows that they typically have a tensile strength below 0.1 MPa (14.5 psi) and a tensile strain capacity less than 0.01%. Even slight SFRM delamination will decrease the failure time of the steel, as heat can penetrate through the gaps in the SFRM coverage and then propagate through the steel directly.

As a type of concrete, SFRMs are brittle and perform poorly when it comes to flexural and tensile strength, and therefore have a significant chance of failure during an earthquake. Since fires are common after an earthquake, the failure of SFRMs can prove very costly for building owners; earthquakes not only cause damage to the building and have a propensity for causing fires, they can also cause damage to fire protection systems. This allows the fire more time to grow and cause more damage to a building. If a fire protection system is damaged, then the SFRM becomes the last line of defense for a building; though an interior of a building may be damaged, an SFRM can keep the structure intact long enough for a fire department to extinguish the fire. However, due to both adhesion failures and the brittle nature of SFRMs, they can delaminate from the structure due to the deformation of the steel members they coat. Their delamination causes the SFRM to perform inadequately, which can lead to the collapse of a building. Another study performed by NIST outlines SFRM damage patterns after earthquakes through a series of experimental tests. After being subjected to cyclic loads (as a way of simulating an earthquake), the following conclusion was made [5]:

“Damage patterns in SFRM for moment frame structures subjected to earthquake deformations were identified. At story drifts of 3 to 4%, SFRM damage was concentrated in the beam flanges where large inelastic deformation and local buckling occurred. Yielding in the assemblage was present at drifts of 1%. The SFRM damage expected at this drift level is limited to debonding of the SFRM at locations where the steel yields.”

As shown by this passage, small amount of deformation in steel can cause the failure of an SFRM due to ineffective bonding between the concrete and the steel. In this study, delamination of SFRMs was also studied from a thermal perspective and showed that SFRM failures will lead to increased steel member temperatures when subjected to a fire.

1.3 SFRM Performance after Partial Delamination

Because of their tendency to delaminate after heavy impact or earthquake events, NIST has studied the performance of SFRMs after they have partially delaminated from the steel members they are covering. A summary of the results are shown in Figure 1.3 below [6].

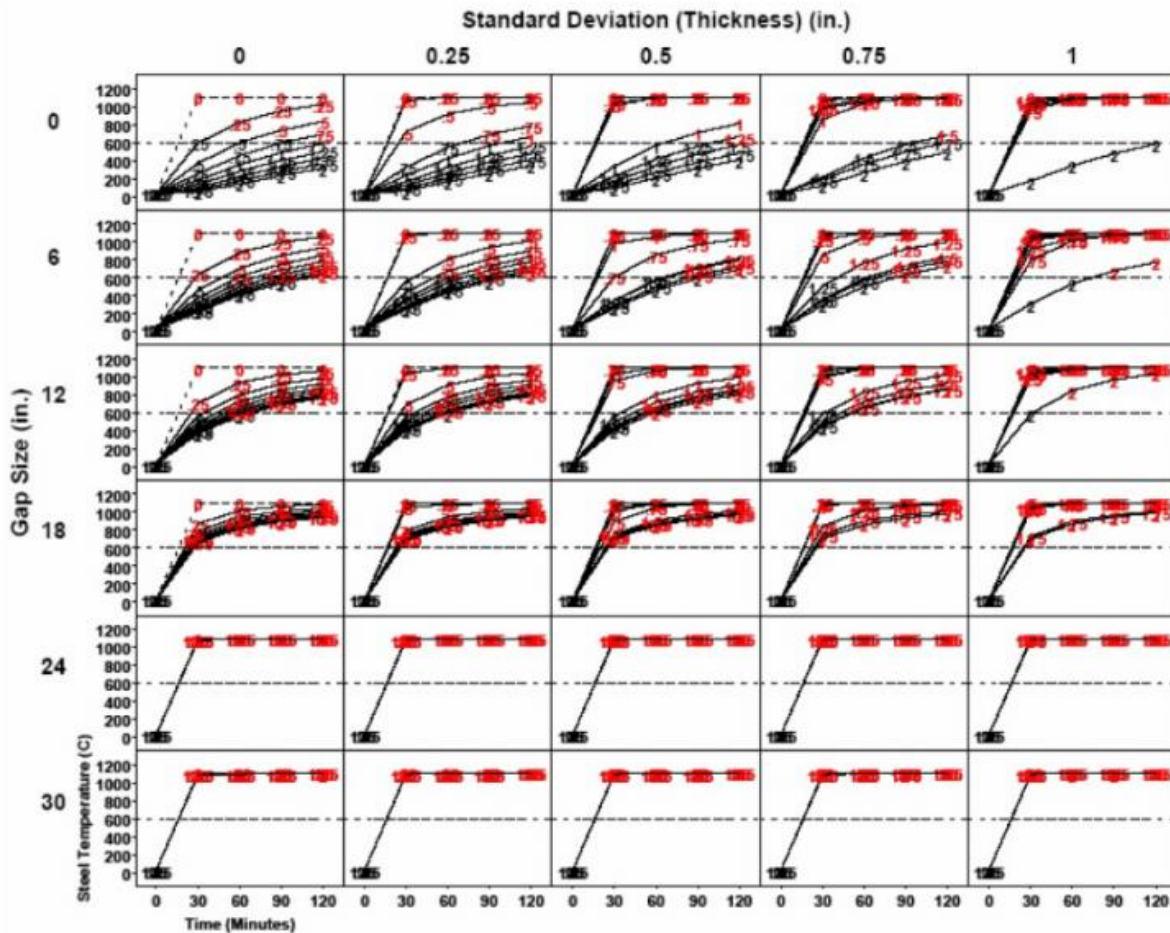


Figure 1.3 [6] shows the relationships between gap size between the SFRM and steel and the temperature of steel over time.

In the figure above, steel temperatures exceeding the maximum allowable value (600°C) are colored in red and temperatures below this threshold are shown in black. In general, these results show that a gap between an SFRM and the steel can cause the entire structure to heat up, which could cause a collapse of the structure due to the weakening of the steel. As expected, a small gap between the steel and SFRM causes the steel to heat up

slower when compared to a large gap between the two materials. A gap size exceeding 18” caused the steel to exceed the maximum safe temperature in less than 30 minutes for each test, regardless of the standard deviation thickness.

A similar study was performed on the effects of partial delamination due to plastic deformation of steel during earthquakes and explosions. The study concluded that 25% delamination of the SFRM can reduce failure time up to 36% (from 100 minutes to 64 minutes). The study mentions that the structure is likely to collapse due to flexural and shear failure in beams near columns.

The same study researched the effects that explosions have on delamination of SFRMs from steel and the effects that fire has on the partial delamination they cause [7]. Similar to the study described above, a structure that experiences 25% delamination of the SFRM will see failure 31% earlier (85 minutes compared to 120 minutes) than a structure that does not experience any delamination of SFRMs.

Although SFRMs can still partially perform their task when partially delaminated, their performance is considerably hindered. Due to failure of the material due to adhesion of the SFRM to the steel or a failure of the material itself due to service loads, there is more optimizing to be done in order to improve properties of SFRMs.

1.4 Introduction to Thermal Conductivity in Concretes

Heat transfer through solid materials is dictated by its thermal conductivity at steady state and by specific heat capacity and density during its transient phase. Specifically in concrete, heat transfer is also controlled by the chemical reactions that occur in the transient phase, as water will dissociate and evaporate when exposed to high temperatures.

The presence of porosity, which is an effect of the low density of an SFRM, reduces the cross sectional area through which heat can be transferred. Therefore, low density of an SFRM (between 240 and 640 kg/m³ compared to over 2,000 kg/m³ for normal structural concretes) is beneficial not just because of the low loads it adds to the structure, but also because of the low thermal conductivity it provides as a result of its porosity.

In order to calculate the thermal conductivity or density of a porous material, the rule of mixtures can be used. This rule states that the properties of a composite material (air-concrete in this example) is a weighted average of the properties of the individual components. A general formula for this expression is below:

$$n^m = \sum_i^N x_i n_i^m$$

In this formula, n is the composite material property, m is an experimentally derived exponential factor, x_i is the volume fraction of the component i , and n_i is the property of component i . Using comparisons to commercially available foam concretes, the exponent m can be approximated as 3/2. Because the thermal conductivity of the air phase can be approximated as zero, the following expression can be used to approximate thermal conductivity of porous cementitious materials:

$$k = k_m(1 - p)^{\frac{3}{2}}$$

In this formula, k_m is the thermal conductivity of the cement matrix, which can be approximated as 1 W/mK, and p is the porosity of the concrete.

Density of the concrete can be determined in a similar fashion; the main difference between the two formulas is the exponential factor: m for density calculations is equal to 1. The following expression can be used to approximate the density of porous cementitious materials (the density of air is approximated as zero for the purpose of simplicity):

$$\rho = \rho_m(1 - p)$$

In this formula, ρ_m is the density of the concrete. These two formulas can then be plotted to find an approximation for the thermal conductivity of the concrete at room temperature in relation to its density.

1.5 SFRM Standardized Performance Tests

SFRM properties are tested and regulated by a series of ASTM tests to assess its material properties. A list of the tests is below:

- ASTM E605/E605M-93(2015): Standard Test Methods for Thickness and Density of Sprayed Fire-Resistive Material (SFRM) Applied to Structural Members [8]
- ASTM E736/E76M-00(2015): Standard Test Method for Cohesion/Adhesion of Sprayed Fire-Resistive Materials Applied to Structural Members [9]
- ASTM E759/E759M-92(2015): Standard Test Method for Effect of Deflection on Sprayed Fire-Resistive Material Applied to Structural Members [10]
- ASTM E760/E760M-92(2015): Standard Test Method for Effect of Impact on Bonding of Sprayed Fire-Resistive Material Applied to Structural Members [11]
- ASTM E761/E761M-92(2015): Standard Test Method for Compressive Strength of Sprayed Fire-Resistive Material Applied to Structural Members [12]
- ASTM E859/E859M-93(2015): Standard Test Method for Air Erosion of Sprayed Fire-Resistive Materials (SFRMs) Applied to Structural Members [13]

- ASTM E937/E937M-93(2015): Standard Test Method for Corrosion of Steel by Sprayed Fire-Resistive Material (SFRM) Applied to Structural Members [14]

Along with tests of its material properties, it is also important to test the material's thermal performance. To test for the thermal conductivity of a material, ASTM E119 is used. The SFRM is exposed to a standard temperature-time curve (shown in Figure 1.4) while the temperature is monitored in specific places (shown in Figure 1.5).

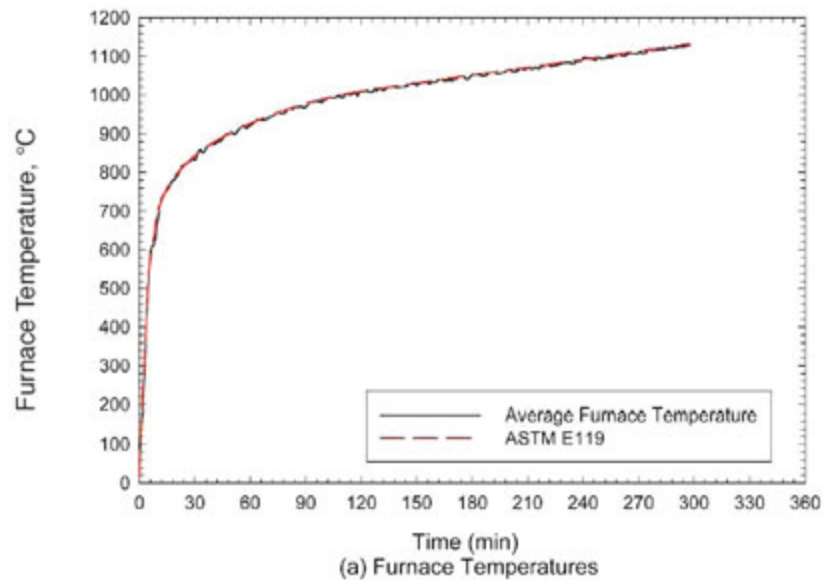


Figure 1.4 [15] shows the standard temperature-time curve used in ASTM E119.

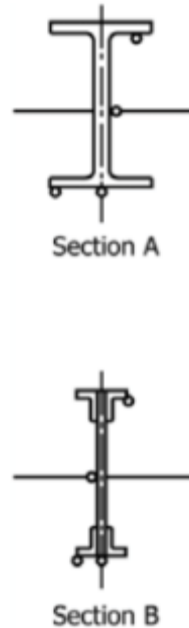


Figure 1.5 [15] shows the locations of the thermocouples used to detect temperature of the steel in ASTM E119.

Its temperature is then compared to the maximum temperature value at which steel is still structurally safe to use. According to this test, the average temperature of the steel shall not exceed 538°C and the maximum temperature of the steel at any one point shall not exceed 649°C. The material and thermal testing of the SFRM helps to determine which SFRM is going to perform the best under certain conditions.

1.6 Introduction to Fiber Reinforced Concrete (FRC)

Concrete's largest downfall is its poor flexural strength. Poor material properties can lead to partial delamination of the SFRM, leading to a more rapid building collapse due to fire. In order to improve its flexural strength, fibers can be added to the concrete mix. Fibers act as a way to control cracking induced by loads on the material or by humidity and temperature variations. The fibers bridge micro-cracks in the matrix at first, and then bridge the distance between cracks when load is applied, which give the concrete post-cracking ductility [16, 17].

There are two main types of fiber reinforced concretes (FRCs): conventional FRCs and high ductility FRCs (also known as Engineered Cementitious Composites, or ECCs). In a conventional FRC, the fibers act as a secondary reinforcement to the concrete. They provide post-cracking ductility, as they bridge the distance between the cracks. However, the stressed held by the fibers between the cracks will be smaller than the stress held by the

fiber bridging the first crack present. Therefore, the material is considered to have a strain-softening behavior [15, 16].

Unlike a conventional FRC, a high ductility FRC has fibers that act as a primary reinforcement to applied loads, which increase ductility and toughness of the material. The materials have a strain hardening behavior when subjected to tension and a deflection hardening when subjected to bending. This means that after the first crack of the high ductility FRC, an additional strain of the composite will require an increase in load. A graph comparing stress-strain curves of normal concrete, conventional FRCs, and high performance FRCs is shown below in Figure 1.6 [16].

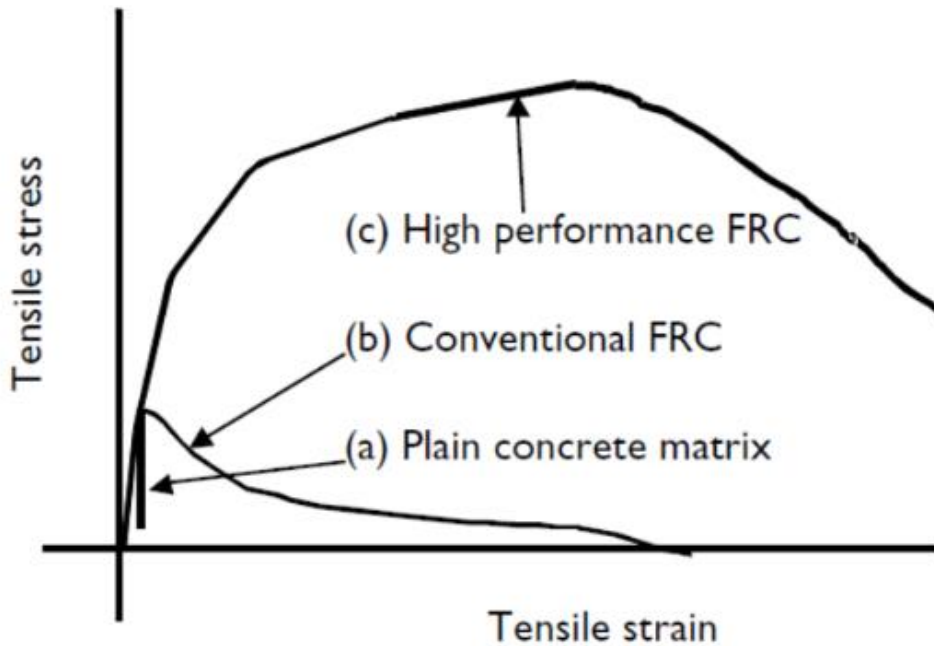


Figure 1.6 [16] shows the relationship between stress and strain in three different types of concretes: normal (no fibers) concrete, conventional FRCs, and high performance FRCs.

Because of the fibers added to high performance FRCs, their strain capacities can reach anywhere between 3% and 7%, multiple orders of magnitude greater than normal concretes. A more specific stress-strain relationship for a high performance FRC is below in Figure 1.7 [15, 16].

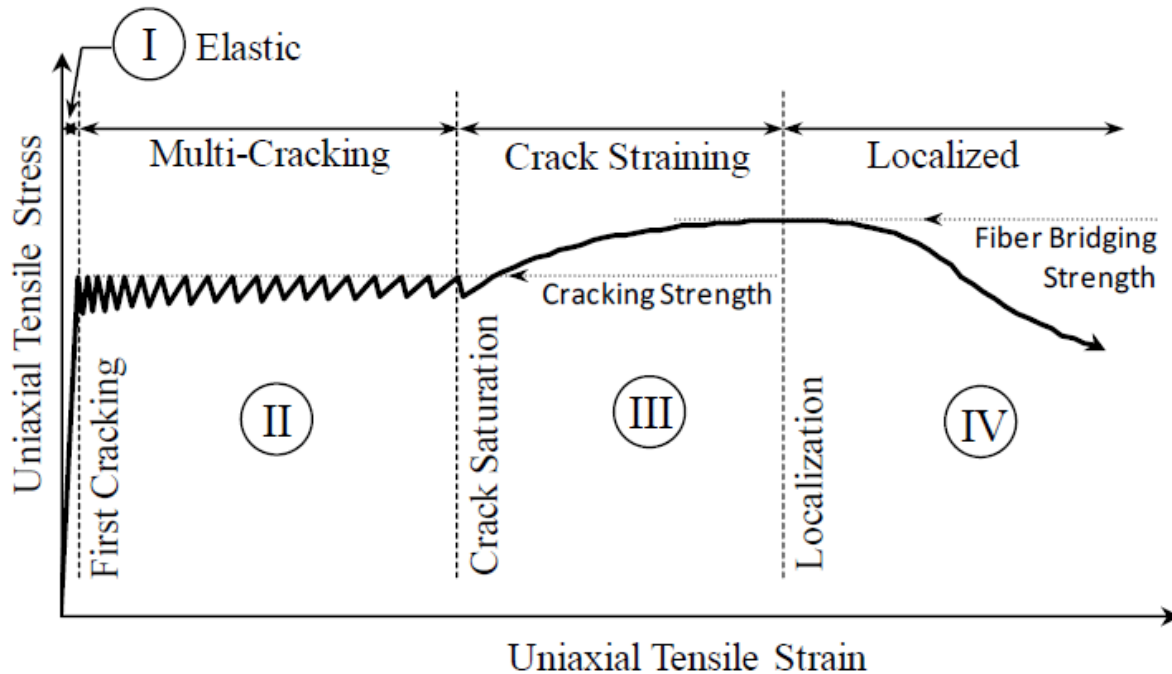


Figure 1.7 [15] shows the stress-strain relationship for a high performance FRC.

A stress-strain curve for a high performance concrete has four phases. Phase I is the standard elastic relationship shown in all materials. Phase I transitions to Phase II after the first crack in the concrete. In a standard concrete, the curve would drop off steeply at this point, as the poor ductility of concrete would cause it to break almost instantly after the first crack. However, in a high performance fiber-reinforced concrete, the fibers begin to take the load applied. As the strain increases, the fibers resist the load until a certain point, where another crack develops in the concrete. However, because of the high strength of the fibers, the crack's size is limited. The fibers once again bridge the span of the crack and hold the load being applied on the SFRM. The multiple cracking continues until the amount of cracks reaches a maximum value. At this point, as the strain increases, the fibers alone are taking the applied load. All of the fibers are now undergoing stress. Phase III shows only an increase in stress as strain increases, as the fibers are undergoing an elastic relationship until entering plastic deformation until quickly cracking. Phase III transitions to Phase IV when the fibers bridging one crack begin to lose significant strength, as many of the fibers are entering plastic deformation or have already snapped.

High performance FRCs have been studied previously for their possible use as SFRMs with promising results [18, 19]. A high performance FRC has been developed with a density of 550 kg/m^3 , which keeps it in the medium density range. It also had a tensile strength of 0.87 MPa (an order of magnitude greater than standard concrete) and a strain capacity of 1% (two orders of magnitude greater than standard concrete). Along with

Improving Ductility of Sprayed Fire Resistant Materials

enhanced material properties, the thermal properties of the potential SFRM are comparable to other SFRMs currently available. However, there is still many improvements to be made to existing SFRM mix design in order to improve its material properties, thermal properties, and adhesion to steel.

2.0 Concrete Materials

Aside from water and ordinary portland cement, there are three materials that need to go into an improved SFRM mix: lightweight aggregates, fibers, and a binding agent (sodium bentonite).

2.1 Lightweight Aggregates

Lightweight aggregates help to reduce the density of the SFRM. They also play a major role in the thermal performance of the SFRM. A table of possible options for lightweight aggregated are shown in Table 2.1 below.

Table 2.1 – Lightweight Aggregate Properties				
Aggregate	Size Range (mm)	Bulk Density (g/mL)	Apparent Density (g/mL)	Water Absorption (mass%)
3M Glass 5-38	0.015-0.075	0.17	0.38	0
Poraver 01.1-0.3	0.1-0.3	0.4	0.85	22
Poraver 0.25-0.5	0.25-0.5	0.34	0.68	15
Poraver 0.5-1.0	0.5-1.0	0.27	0.45	9
Poraver 1.0-2.0	1.0-2.0	0.23	0.41	7
Vermiculite Grade 1	Grade 1	0.135	0.18	180

Table 2.1 shows the size, densities, and water absorption properties of lightweight aggregates that may be used in an SFRM mix.

Vermiculite has a different size distribution than the rest of the possible lightweight aggregates, as the vermiculite pellets have a relatively large range of potential size. Below, in Figure 2.1, is a graph of the size distribution of vermiculite.

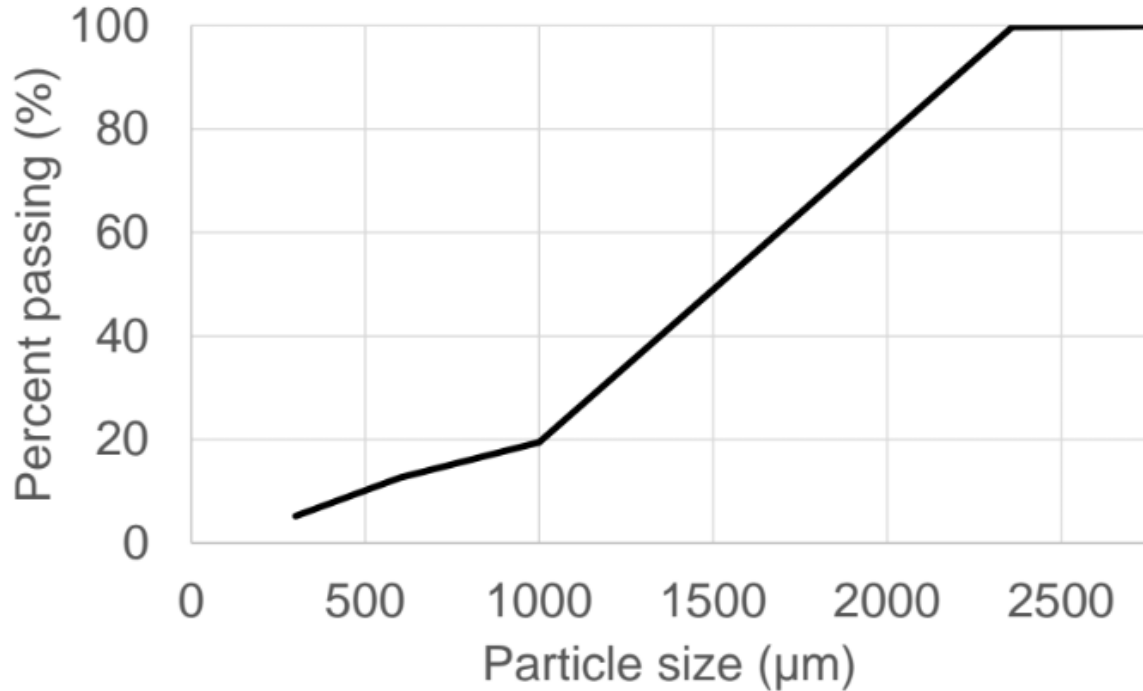


Figure 2.1 shows the distribution of vermiculite pellet size.

Vermiculite is a very lightweight aggregate with a porous structure and high capacity for water absorption. It is most frequently used in cement based SFRMs because of its low weight, low thermal conductivity, low cost, and stability at high temperatures. The vermiculite used in SFRMs is considered to be a wet aggregate. Before mixing, the vermiculite is typically soaked in water so that reaches its absorption limit with some water leftover, putting it past saturated-surface dry conditions. Vermiculite is also a good option for use in SFRMs because it can counteract shrinkage and reduce thermal contraction strains at high temperatures.

Though they are often seen as an inert filler, aggregates play an important role in the mixing of concrete. Aggregates do act as a way to increase the volume of a concrete so that it does not just consist of cement and water. Vermiculite especially helps with this, as it has a very low density; its low density allows the addition of a high volume of vermiculite into the mix without increasing the weight of the mix, which therefore lowers its volume. However, aggregates like vermiculite can positively effect a concrete's thermal conductivity. Vermiculite boasts a low thermal conductivity (~ 0.06 W/mK), so it has favorable effects for an SFRM trying to prevent the increase in temperature of the steel it is protecting. An aggregate's texture can also effect the workability and strength of the concrete. An aggregate with a smooth surface improves the workability of a fresh concrete, though its relatively low surface area gives the concrete paste less room to bind to – this reduces the strength of the concrete when compared to an aggregate with a rough surface. The opposite is true for an aggregate like vermiculite with a rough surface. Though the

workability of a concrete with vermiculite is relatively lower, the concrete is relatively stronger because of the greater bonding surface area between the aggregate and the cement paste.

2.2 Fibers

Nylon fibers are used in a wide range of applications because of their favorable material properties. Nylon fibers perform well when it comes to strength, abrasion, toughness, and fatigue resistance. In previously studied concretes, nylon fibers have been shown to increase ductility. Fibers like polypropylene are chemically stable in the alkaline cement environment, leading to its longevity.

The cement/fiber interface created by fibers like PVA, polypropylene, and nylon, as well as the resulting adhesion energies, have been previously studied using atomistic simulation and experimental techniques. The functional group in the structure of the polymer macromolecules was shown to affect the adhesion energy primarily by changing the C/S ratio of the C-S-H interface and by absorbing additional positive ions in the C-S-H structure. Of the three types of fibers tested, nylon showed better adhesion energies than both polypropylene and PVA.

Although nylon has lower tensile strength and frictional sliding shear stress when compared with PVA and HTPP, nylon will be used for the purpose of this study. The use of nylon is justified by the specific nature of the composite material. It has a low density matrix of inherently lower strength than most cementitious applications. Also, the elastic modulus of the material allows for larger crack width opening at lower values of maximum bridging stress. A larger crack width contributes to an increased ductility of the final SFRM. A table of pertinent material properties of the fibers is shown below in Table 2.2.

Table 2.2 – Nylon Fiber Characteristics	
Length – L_f (mm)	12.7
Diameter – D_f (μm)	12
Tensile Strength – σ_f (MPa)	660-1080
Strain to Failure – ϵ (%)	15-30
Elastic Modulus – E (GPa)	3.0-5.4

Table 2.2 shows material properties of the nylon fibers used in the SFRM mix design.

2.3 Sodium Bentonite

Sodium bentonite is used as a filler material in the concrete mix to provide insulation properties as well as workability to the mix. Bentonites are commercially

available pozzolans composed of smectite clay materials; its main components are silica and alumina arranged in sheet-like units. Their surface characteristics and cation exchange capacity cause the adjacent water molecules to behave different from normal water, which improves the viscosity, thixotropy, and plasticity of the mix. Sodium bentonite is capable of adsorbing multiple times its dry mass in water, which forms a colloidal mixture with a high viscosity; this makes it good to add to the mix because it aids its workability as well as aids in fiber dispersion. Bentonite clays have previously been used in cementitious applications as a low cost pozzolan to partially replace ordinary portland cement. The makeup of sodium bentonite by chemical compound is shown below in Table 2.3.

Table 2.3 – Sodium Bentonite Properties	
Chemical Compound	% (by weight)
SiO ₂	66.05 – 71.86
Al ₂ O ₃	20.32 – 26.03
Fe ₂ O ₃	2.95 – 4.65
MgO	2.35 – 3.66
CaO	< 0.23

Table 2.3 shows the breakdown of chemical compound by weight in sodium bentonite.

In this study, a sodium bentonite from the Wyoming (USA) region was used. 90% of its particles are finer than 150 microns and 35% finer than 75 microns. It disperses in water to form large yet very thin flakes, providing colloidal, plastic, and bonding properties.

3.0 Methods

There were three steps in the testing performed on the SFRM. The first step was to formulate an optimal mix design using the materials outlined in the previous chapter and creating the concrete specimen. Once they were cured, the specimens underwent mechanical testing to assess their flexural efficacy.

3.1 Concrete Mix Design

Five different concrete mixes were tested over the course of this study. The three mixes, listed below in Table 3.1, have the same amounts of fibers, cement, vermiculite, and sodium bentonite; they vary in the amount of water present in the mix. All materials are listed in terms of pounds per pound of cement besides fibers, which is listed by a volume percentage.

Mix ID	Cement	Water	Vermiculite	Sodium Bentonite	Fibers
1	1.0	1.89	0.14	0.18	1.7%
2	1.0	1.69	0.14	0.18	1.7%
3	1.0	1.49	0.14	0.18	1.7%
4	1.0	1.29	0.14	0.18	1.7%

The vermiculite and sodium bentonite were soaked in 325% and 10% their mass in water respectively for 24 hours before mixing. The mixing process was as follows:

1. The dry materials were combined (cement, vermiculite, sodium bentonite) and mixed for 3 minutes at stir speed (60 rpm). The sides of the bowl were scraped down so no materials stayed on the side of the bowl.
2. The water was added to the bowl and mixed for 2 minutes at 100 rpm. The sides of the bowl were scraped down so no materials stayed on the side of the bowl.
3. The fibers were gradually added to the mix while it was mixed for 2 minutes at 100 rpm. The sides of the bowl were scraped down so no materials stayed on the side of the bowl.
4. Lastly, the combined materials were mixed for 2 minutes at 200 rpm.

The concrete was then put into 63.5 mm x 254 mm x 38 mm for a day. They were then removed from their molds and continued to cure for two weeks.

3.2 Mechanical Testing

Mechanical properties of the SFRMs were assessed using four point bending tests. Using the samples measuring 63.5 mm x 254 mm x 38 mm, the SFRM was loaded with a span length of 240 mm and a loading span of 80 mm, one-third of the span length. The test was conducted under a displacement of 1.4 mm/min.

3.3 Computation of Stress-Strain Curves

Upon testing the specimens under a 4-point bend, the software outputs raw data in the form of a load/displacement curve. Using the load (F) and the displacement (δ), the stress-strain curve can be computed. Flexural stress is defined as $\sigma = \frac{Mc}{I}$, where M is the moment on the sample, c is the distance from the neutral axis to the top of the sample (which, in the case of a rectangular cross section, is half of the height) and I is the moment of inertia for the sample, which is equal to $\frac{bh^3}{12}$. Due to the loading characteristics of the sample, the moment on the specimen is equal to $\frac{Fd}{2}$, where d is the distance from the support to the point at which the force is acting. By inputting values for the variables in the original stress equation ($\sigma = \frac{Mc}{I}$), the final equation for stress is $\sigma = \frac{3Fd}{bh^2}$. Each variable in this equation is known due to the geometry of the test besides F , which is outputted by the test software. Figure 3.1 shows the location and definitions of the variables used in calculating the stress on the beam.

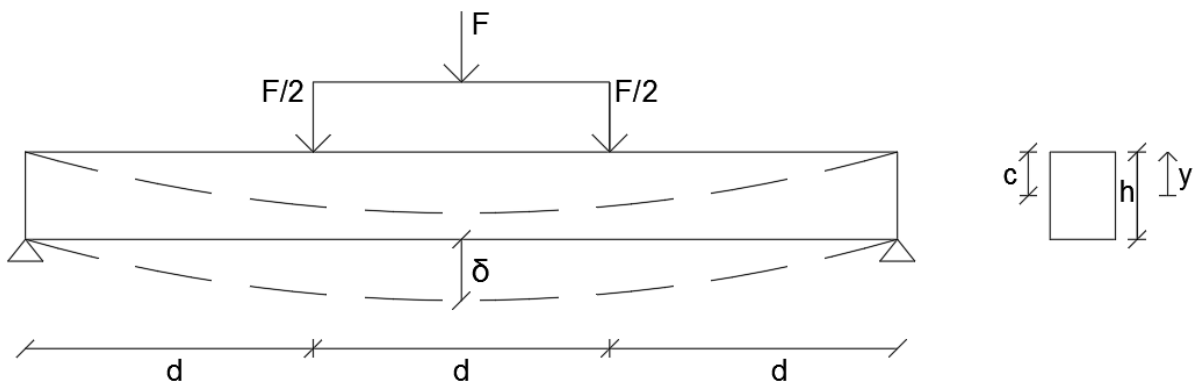


Figure 3.2 defines variables used in calculating the strain on the specimen under a four-point bend test.

Strain is defined as strain divided by elastic modulus ($\epsilon = \frac{\sigma}{E}$). However, the software used to perform the test does not give an exact value for elastic modulus, it can only approximate it. In order to get a more accurate value for strain, we can use the diagram in Figure 3.2.

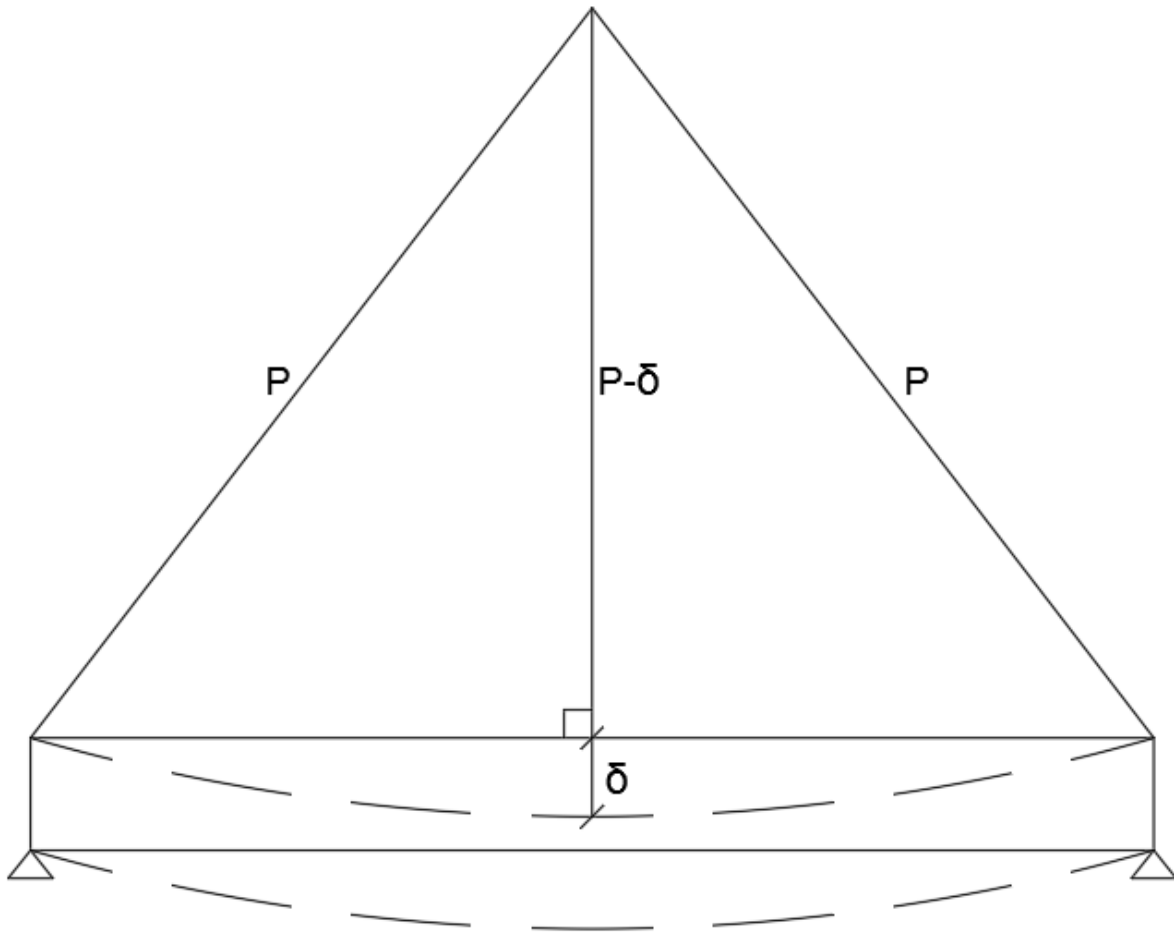


Figure 3.2 defines variables used in calculating the strain on the specimen under a four-point bend test.

The deformed shape of the bowed specimen can be modeled as an arc that has a certain radius P . The distance from the origin of the circle O to any point on the beam is equal to the radius P . On the ends of the beam, there is no deflection. In the middle of the beam, the radius is still P , but the deflection can be defined as δ . Therefore, a right triangle can be made with legs L and $(P - \delta)$, and hypotenuse P , where L is half the length of the beam. Using the Pythagorean Theorem, $(P - \delta)^2 + L^2 = P^2$. This equation can be rearranged to make $P = \frac{L^2}{2\delta}$. Strain can be calculated using $\epsilon = \frac{y}{P}$, where y is the distance from the

neutral axis to the top of the specimen. The value of P can be substituted for in this equation and, with some rearranging and substitutions, a final equation for strain can be derived: $\varepsilon = \frac{h\delta}{L^2}$. Using these two equations, a stress-strain can be computed using just the force and displacement output from the testing software.

4.0 Results

The following figures display stress-strain curves for the four mixes synthesized over the course of the project. The curves vary in magnitude but follow a similar pattern which can be separated into four different phases. Phase I shows a linear relationship between stress and strain representative of an elastic material. Phase II shows a rapid drop-off of stress present in the material due to the first crack in the specimen. Phase III shows the elastic straining of the crack, where the fibers hold the stress generated by the load on the specimen. There is a slight increase in the stress that can be held by the fibers during this phase. In Phase IV, the fibers begin to plastically deform and rupture, which explains the gradual drop-off in flexural stress that can be withstood by the beam. Because the specimen would not abruptly fracture like a conventional, non-fiber reinforced concrete, the test was halted when the specimen held 25% of the maximum load held in the course of the test.

4.1 Mix 1 Results

In total, 5 specimens were tested for each mix. 2 specimens were tested after 1 week of curing, while the other 3 specimens were tested after 2 weeks of curing. Figure 4.1 shows the stress-strain curves for Mix 1, which had a 1.89 W/C ratio.

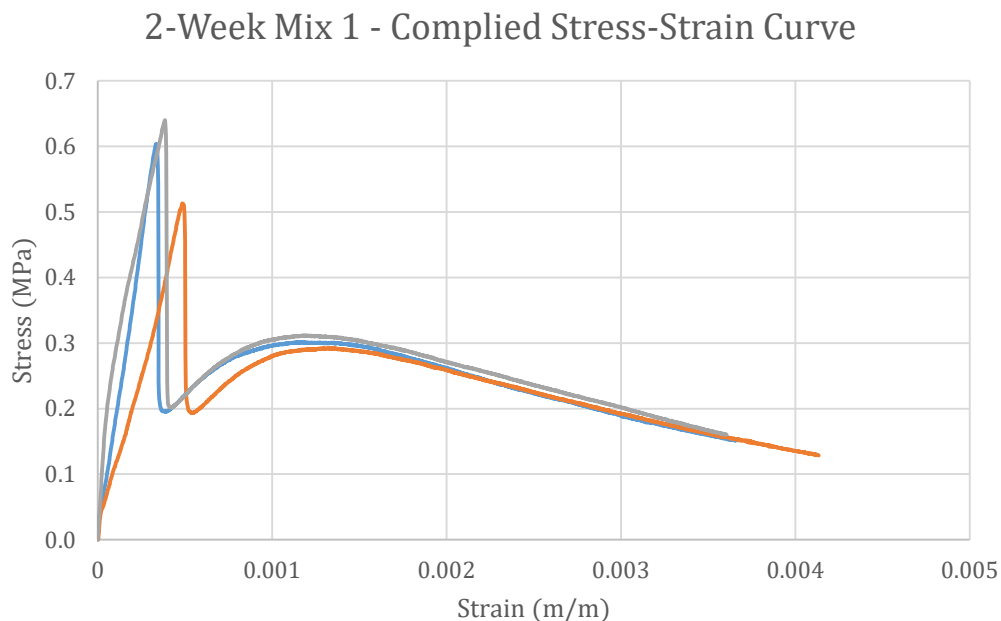


Figure 4.1 shows stress-strain curves for Mix 1, tested at both 1 week and 2 weeks of curing.

After 2 weeks of curing, the average first crack strength of the specimen was 0.585 MPa. In the 2-week strength test, though the specimens reached first crack strength and slightly different stresses, the post-cracking strength were almost exactly the same; each specimen was able to hold approximately 0.2 MPa after the first crack. The stress on the sample then increased up to a fairly consistent value of ~0.3 MPa before entering Phase IV, where the fibers begin to deform plastically and rupture, leading to the decrease in stress capacity towards the end of the test. On average, the first crack occurred at 0.0403% strain on the specimen. The specimen still held 25% of its maximum load at strain levels as high as 0.380% strain. After curing for two weeks, the density of Mix 1 was 0.894 g/cm³.

4.2 Mix 2 Results

Figure 4.2 shows the stress-strain curves for Mix 2, which had a 1.69 W/C ratio.

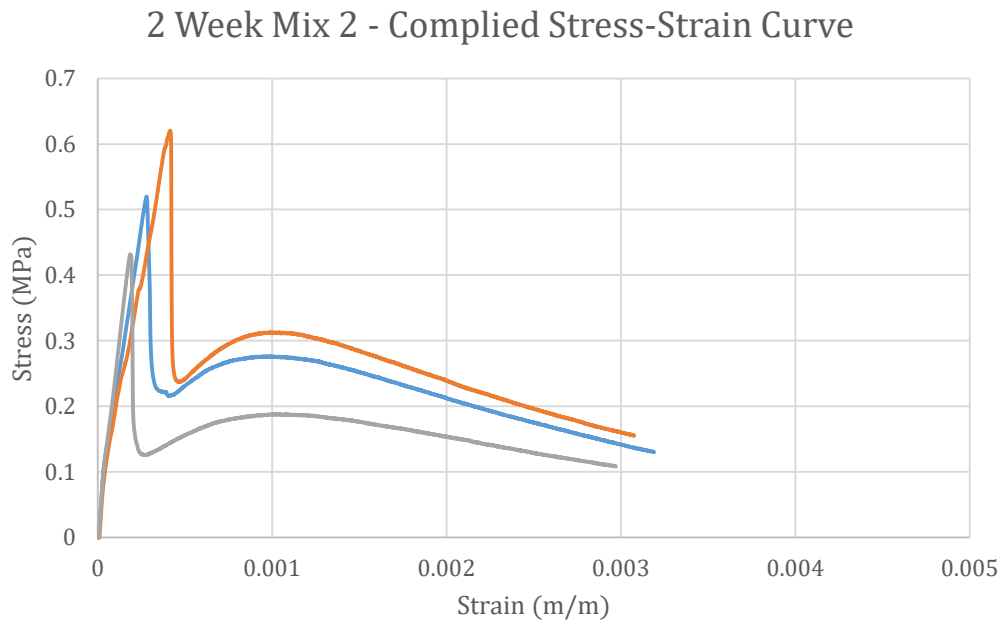


Figure 4.2 shows stress-strain curves for Mix 2, tested at both 1 week and 2 weeks of curing.

Figure 4.2 shows that the first-crack strength of the concrete after 2 weeks of curing averages to be 0.523 MPa. The graph follows the same general model of elastic deformation, steep drop-off of stress capacity after initial cracking, gradual increase of stress capacity as fibers elastically deform, and gradual decrease as fibers plastically deform and rupture. On average, the first crack occurred at a strain of 0.0293%. The specimen held 25% of its maximum load at strain levels of 0.307% on average. After 2 weeks of curing, 0.996 g/cm³.

4.3 Mix 3 Results

Figure 4.3 shows the stress-strain curves for Mix 3, which had a 1.49 W/C ratio.

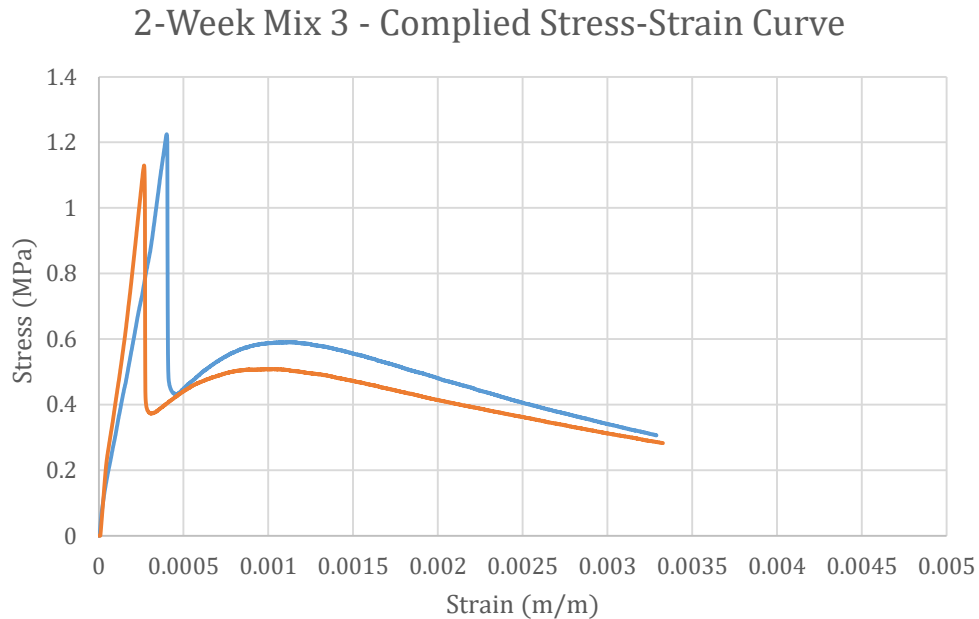


Figure 4.3 shows stress-strain curves for Mix 3, tested at both 1 week and 2 weeks of curing.

After 2 weeks of curing, the average first crack strength was 1.180 MPa. Stress capacity after first crack decreased to approximately 0.4 MPa. A decrease to a fairly constant value after initial cracking is logical. Though first crack strength is expected to increase as concrete cures, the post-crack strength is expected to be approximately equal regardless of curing time. This is due to the fact that fibers hold the load in this phase, and fiber strength does not vary with curing time. Both samples tested output a stress-strain curve consistent with the four phase model described above (elastic deformation of concrete, initial cracking, elastic deformation of fibers, plastic deformation and rupture of fibers). First crack strength occurred at 0.0334% strain on average. The specimen still held 25% of its maximum load at strain levels of 0.331%. After 2 weeks of curing, the density of the mix was 1.059 g/cm³.

4.4 Mix 4 Results

Figure 4.4 shows the stress-strain curves for Mix 3, which had a 1.29 W/C ratio.

2-Week Mix 4 - Compiled Stress-Strain Curve

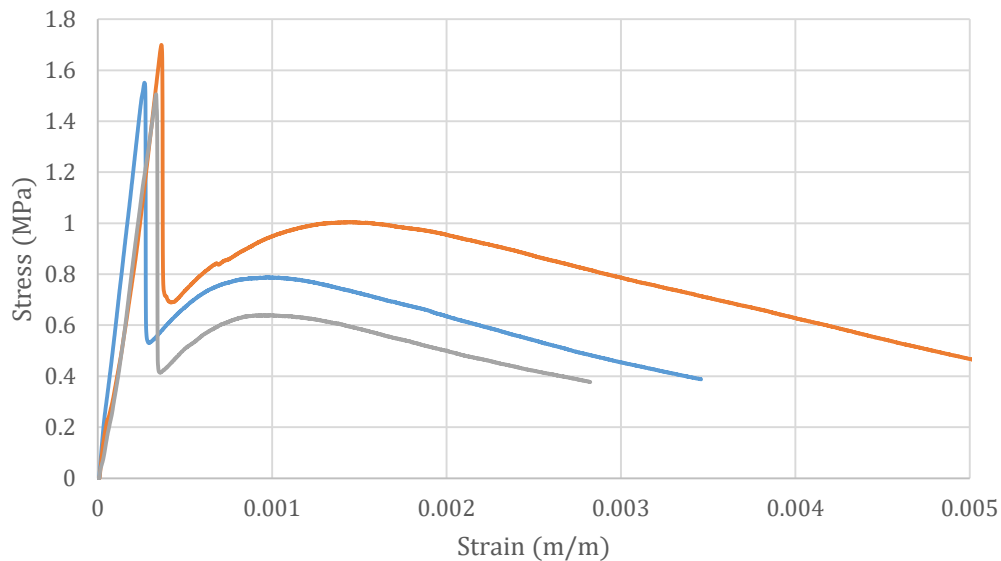


Figure 4.4 shows stress-strain curves for Mix 4, tested at both 1 week and 2 weeks of curing.

The 2-week tests show that the average first crack of the concrete was 1.575 MPa. All three graphs are consistent with the four-phase model for the synthesized SFRM described above. On average, the initial crack in the concrete occurred at a strain level of 0.0322%. The maximum strain held by the specimen at the end of the test was 0.385%. The density of the mix after 2 weeks of curing was 0.894 g/cm³.

4.5 Results Summary

In general, most specimens tested followed a logical progression of elastic deformation of the concrete, a steep decrease in stress capacity directly after a first crack, elastic deformations of fibers, and plastic deformation of fibers. There were some specimens tested that did not follow this model exactly, which can be explained by the nonhomogeneous nature of concrete. A summary of the results are displayed in the Table 4.5.

Table 4.5 – Summary of Specimen Strength and Density				
Mix ID	Avg. First Crack Stress (2-Week) (MPa)	Strain at First Crack	Maximum Strain	Density (kg/m ³)
1	0.585	0.0403%	0.380%	0.894
2	0.523	0.0293%	0.307%	0.966
3	1.180	0.0334%	0.331%	1.059
4	1.575	0.0322%	0.385%	1.183

These results are consistent with established research that flexural strength increases and density increases as W/C ratio.

5.0 Discussion

5.1 Mechanical Results Discussion

Each of the four mixes tested displayed properties far better than traditional SFRMs that are not fiber reinforced. Commercially available SFRMs have tensile stress capacities of less than 0.1 MPa and a strain capacity of 0.01%. Conversely, the four mixes tested had tensile stress capacities between 0.523 and 1.575 MPa, or about 5x to 16x greater than currently available SFRMs. The specimens also had first crack strains between 3x and 4x greater than standard SFRMs. Due to the addition of fibers to the mix, the specimens were able to resist strains between 0.307% and 0.385%, more than two orders of magnitude greater than standard SFRMs. In this sense, the mechanical properties of SFRMs were greatly improved upon.

However, mechanical results were not optimized. An ideal SFRM would share its characteristics with a high performance FRC, which possesses strain hardening behavior. After the first crack, the sharp decrease in stress capacity would not be large in magnitude and the fibers that bridge the crack would be able to hold enough stress to the point that the concrete would crack elsewhere. Continuous cracking would occur until a crack saturation point is reached, at which point the fibers plastically deform and rupture. Instead of a high performance FRC, the results obtained from testing the four specimens were more comparable to stress-strain curves of a conventional FRC. Conventional FRC's typically undergo one crack when subjected to a high enough magnitude of load. After cracking, the decrease in stress capacity is relatively large. The fibers that bridge the initial crack cannot elastically deform enough to bring the stress capacity back up to the cracking strength. Instead, they will fail before that, which leads to the gradual decrease in stress capacity.

In order to achieve strain-hardening behavior present in a high performance FRC, the mix design would have to be modified. An increase in fibers by volume would likely contribute to or solve the issue of strain-softening behavior present in all four mixes tested. The addition of more fibers increases the cross section of fibers that can hold stresses induced by loading on the beam, which would help to minimize the drop in stress capacity after the first crack. This would thereby decrease the amount of elastic deformation needed to rise back up to the cracking strength of the concrete. Other than modifying the amount of fibers in the mix, the amount of sodium bentonite may need to be adjusted slightly. Because it aids in fiber dispersion throughout the mix, additional sodium bentonite may need to be added to account for the additional fibers added. It would also help to minimize any imperfections or anomalies present due to uneven distribution of fibers, as concrete is inherently nonhomogeneous.

5.2 Expected Thermal Results Discussion

Due to the fact that concrete is a nonhomogeneous mixture of different materials, its thermal conductivity varies at different temperatures; this is different from many materials that have fairly constant thermal conductivity over large ranges of temperatures. The thermal conductivity of the SFRM is expected to rise linearly for low temperatures, but begin to decrease at 100°C (the evaporation point of water). Thermal conductivity is expected to decrease even more so up to 300°C, where thermal conductivity is very close to zero. This is due to an endothermic process at 300°C which results from heat absorption due to continuous water evaporation from the cementitious matrix [20]. After the steep drop to almost zero, the thermal conductivity linearly increases. This is due to multiple factors. Porosity of the SFRM is constantly increasing due to the evaporation of water from the cementitious matrix as well as the melting and vaporization of the nylon fibers. Nylon fibers are expected to vaporize at approximately 340°C, which further increases porosity. Increasing porosity allows for more radiative heat transfer through the voids left in the concrete. Because radiation is proportional to the fourth power of temperature, the magnitude of heat transfer through recently made pores contributes to the rising thermal conductivity of the SFRM at higher temperatures. An increase in thermal conductivity can also be contributed to the effects that high temperatures have on cement. At high temperatures, the crystallinity of gypsum increases [20]. As crystallinity increases, the thermal performance of the cement (and therefore the entire specimen) deteriorates. Anomalies in the linear increase are expected at 550°C and 620°C, as exothermic dissociation reactions of C-S-H take place at those temperatures.

Addition of additional fibers into the mix as proposed above would only serve to worsen thermal performance of the SFRM [21]. An increase in fiber volume would lead to increased porosity in the SFRM. Because of this, thermal testing would need to be performed in an attempt to optimize both mechanical performance (high performance FRC stress-strain curves) and thermal performance (limiting porosity by keeping fiber volume to a minimum).

6.0 Conclusion

A new sprayed fire resistant material has been made using ordinary portland cement, water, vermiculite, sodium bentonite, and nylon fibers. Mechanical properties of four different mixes were tested via a four-point bend test. By introducing nylon fibers into the concrete, the first crack strength and strain capacity of the concrete were increased by one and two orders of magnitude, respectively. Each sample tested followed a similar progression to failure: elastic deformation of the concrete, cracking of the concrete, elastic deformation of the fibers holding tensile stress, and plastic deformation/rupture of the fibers. Unfortunately, the specimens tested displayed strain-softening behavior, which is representative of a conventional FRC. Future testing should be performed on the SFRM in an attempt to optimize the mix in order to develop a strain-hardening behavior that is characteristic of a high performance FRC. This will most likely be performed by increasing the amount of fibers by volume present in the concrete.

7.0 References

1. Outinen, J., & Mäkeläinen, P. (2004). Mechanical properties of structural steel at elevated temperatures and after cooling down. *Fire and Materials*, 28(24), 237-251.
doi:10.1002/fam.849
2. Isolatek International. (2017). Fireproofing – Commercial Density Wet Mix SFRM CAFCO 300. Retrieved April 19, 2018, from <http://isolatek.com/cd-c300/>
3. Society of Fire Protection Engineers. (2016). *SFPE Handbook of Fire Protection Engineering*. New York: Springer.
4. NIST NCSTAR (2005). Collapse of the World Trade Center Towers. Final Report. Federal Building and Fire Safety Investigation of the World Trade Center Disaster, NIST; National Construction Safety Team, 208.
5. FEMA (2002). World Trade Center Building Performance Study: Data Collection, Preliminary Observations, and Recommendations, Federal Emergency Management Agency (FEMA). Federal Insurance and Mitigation Administration, Washington, DC.
6. Carino, N. J. (2005). *Passive Fire Protection*(pp. 1-328) (United States of America, U.S. Department of Commerce, National Institute of Standards and Technology). Washington DC: NIST.
7. A. Arablouei and K. Venkatesh, "Effect of fire insulation delamination on structural performance of steel structures during fire following an earthquake or an explosion," *Fire Safety Journal*, no. 84, pp. 4049, 2016
8. American Society for Testing and Materials, ASTM E605/E605M-93(2015): Standard Test Methods for Thickness and Density of Sprayed Fire Resistive Material (SFRM) Applied to Structural Members, 2015.
9. American Society for Testing and Materials, ASTM E736/E736M-00(2015): Standard Test Method for Cohesion/Adhesion of Sprayed Fire Resistive Materials Applied to Structural Members, 2015.
10. American Society for Testing and Materials, ASTM E759/E759M-92(2015): Standard Test Method for Effect of Deflection on Sprayed Fire Resistive Material Applied to Structural Members, 2015.
11. American Society for Testing and Materials, ASTM E760/E760M-92(2015): Standard Test Method for Effect of Impact on Bonding of Sprayed Fire Resistive Material Applied to Structural Members, 2015.

12. American Society for Testing and Materials, ASTM E761/E761M-92(2015): Standard Test Method for Compressive Strength of Sprayed Fire Resistive Material Applied to Structural Members, 2015.
13. American Society for Testing and Materials, ASTM E859/E859M-93(2015): Standard Test Method for Air Erosion of Sprayed Fire Resistive Materials (SFRMs) Applied to Structural Members, 2015.
14. American Society for Testing and Materials, ASTM E937/E937M-93(2015): Standard Test Method for Corrosion of Steel by Sprayed Fire Resistive Material (SFRM) Applied to Structural Members, 2015.
15. American Society for Testing and Materials, ASTM E119/E119-18 (2015): Standard Test Method for Fire Tests of Building Construction and Materials, 2015.
16. A. Bentur and S. Mindess, Fiber Reinforced Cementitious Composites, Taylor & Francis, 2007.
17. A. Bentur and S. Mindess, Fiber Reinforced Cementitious Composites, 2007.
18. Q. Zhang and V. C. Li, "Development of durable spray-applied fire-resistive Engineered Cementitious Composites (SFR-ECC)," *Cement & Concrete Composites*, no. 60, pp. 10-16, 2015.
19. Q. Zhang and V. C. Li, "Adhesive bonding of fire-resistive engineered cementitious composites (ECC) to steel," *Construction and Building Materials*, no. 64, pp. 431-439, 2014.
20. Benichou, N. (2001). *Thermal properties of wood, gypsum and insulation at elevated temperatures*(Canada, CNRC, Institute for Research in Construction). Ottawa: Institute for Research in Construction. Retrieved March 18, 2018.
21. Ezziane, M., Kadri, T., Molez, L., Jauberthie, R., & Belhacen, A. (2015). High temperature behaviour of polypropylene fibres reinforced mortars. *Fire Safety Journal*, 71, 324-331. doi:10.1016/j.firesaf.2014.11.022